# Role of elastic deformation in determining the mixed alkaline earth effect of hardness in silicate glasses

Jonas Kjeldsen, Morten M. Smedskjaer, Marcel Potuzak, and Yuanzheng Yue

---

**Articles you may be interested in**

Hardness and incipient plasticity in silicate glasses: Origin of the mixed modifier effect
Appl. Phys. Lett. **104**, 051913 (2014); 10.1063/1.4864400

Activation energy for alkaline-earth ion transport in low alkali aluminoborosilicate glasses
Appl. Phys. Lett. **102**, 082904 (2013); 10.1063/1.4794174

Thermal poling of alkaline earth boroaluminosilicate glasses with intrinsically high dielectric breakdown strength
J. Appl. Phys. **111**, 083519 (2012); 10.1063/1.3703679

Thermodynamics of viscous flow and elasticity of glass forming liquids in the glass transition range
J. Chem. Phys. **135**, 184501 (2011); 10.1063/1.3656695

Electron irradiation induced phase decomposition in alkaline earth multi-component oxide glass
J. Appl. Phys. **92**, 2310 (2002); 10.1063/1.1496148

---

# Role of elastic deformation in determining the mixed alkaline earth effect of hardness in silicate glasses

Jonas Kjeldsen,[1] Morten M. Smedskjaer,[1] Marcel Potuzak,[2] and Yuanzheng Yue[1,a]

[1]*Section of Chemistry, Aalborg University, DK-9000 Aalborg, Denmark*
[2]*Science and Technology Division, Corning Incorporated, Corning, New York 14831, USA*

Glasses deform permanently as a result of indentation and the total resistance to deformation consists of three individual resistances, i.e., those to elastic deformation, densification, and plastic flow. The link between Vickers hardness and the resistances to densification and plastic flow has been investigated previously, but the link between the resistance to elastic deformation and hardness has not yet been studied. In this work, we investigate the link between elastic deformation during indentation and Vickers hardness in a series of mixed magnesium-barium boroaluminosilicate glasses. We show that the mixed alkaline earth effect manifests itself as deviations from linearity in shear modulus, Poisson's ratio, glass transition temperature, liquid fragility index, hardness, volume of densification, and volume of plastic flow. We find no correlation between the elastic part of the indentation and hardness, and we thus infer that elastic deformation does not play a dominant role in determining the mixed alkaline earth effect of hardness. However, interestingly, we find a strong correlation between Poisson's ratio, volume of plastic flow, and hardness, by which the minimum in hardness could be explained in terms of a minimum in shear viscosity. © 2015 AIP Publishing LLC. [http://dx.doi.org/10.1063/1.4906099]

## INTRODUCTION

The study of indentation deformation processes in glass was initiated in 1962, at which time it was proposed that these processes obey the classical law of plasticity, i.e., indentation was perceived as a purely plastic process.[1–4] Later, via comparison between the indent volume and the volume of pile-up, it was shown that indentation deformation originates from both plastic flow and densification.[5–7] It is now widely accepted that intrinsically glass is a brittle material that deforms both by plastic flow and by densification when pressure is applied.[1] As hardness is a measure of the ability for a material to resist elastoplastic deformation, it is one of the most important mechanical properties of glass for applications such as scratch-resistant covers for personal electronic devices.[8]

According to Yamane and Mackenzie,[9] the resistance of a glass to deformation is a result of the resistance to three distinct deformation processes: plastic flow, densification, and elastic deformation. Plastic flow is a volume conservative displacement of matter, where material is forced upwards creating a positive flux, which in turn results in pile-ups around the indent. Densification is a non-volume conservative irreversible compression that creates a hemispherical area of increased density beneath the indent. Elastic deformation is a reversible compression that recovers after unloading. Recently, Yoshida et al.[10] have developed a method that is capable of quantifying the amount of non-plasticity in glass. One of the key steps for the method is to perform sub-$T_g$ annealing to enable quantification of densification and plastic flow. The resistance to the elastic part of the deformation process is, however, not accessed in their

approach.[10–12] Under an applied pressure, the atomic bonds in the glass stretch and bend away from their favorable position, allowing for some elastic deformation. Upon unloading, the bonds return to the state of lowest energy and the material recovers to its original shape. In other words, part of external mechanical energy (given by indentation) causes elastic work in the glass, which in turn leads to an increase of the potential energy of the atoms. When unloading, this increased potential energy is released, resulting in an expansion work. The rest of the mechanical energy causes plastic flow (i.e., a sort of deformation work), permanent densification (a permanent high potential state) and a small amount of dissipation heat. Thus, the energy conservation law is obeyed. As hardness is calculated as the applied force divided by the indent size, part of which is used for the elastic deformation, the latter contributes to the glass hardness.[9,10] Kjeldsen et al.[4,13] have proposed a new approach to predict the compositional scaling behavior of hardness in mixed modifier silicate glasses. In this approach, the compositional dependence of hardness is assumed to be a consequence of the resistance of the glass network to plastic flow. The investigated mixed modifier glass systems were designed to achieve constant elastic moduli with respect to composition, i.e., the influence of the elastic deformation on hardness was kept constant.

The resistance of a glass to permanent deformation (i.e., hardness) is typically dominated by one of the three deformation process. Kjeldsen et al.[4,13] have found that in mixed modifier glasses, the resistance to plastic flow is the dominant resistance to deformation.[4] However, in glass systems of high silica content (>85 mol. % $SiO_2$), densification has been reported to be the dominant deformation process.[4–6,10–14] In certain glass systems indented under low loads, elastic

a)Author to whom correspondence should be addressed. Electronic mail: yy@bio.aau.dk. Tel.: +45 9940 8522.

**117**, 034903-1

deformation could be the dominant deformation process. In order to enable prediction of the compositional dependence of hardness, it is important to account for all three deformation mechanisms. Makishima and Mackenzie considered the glass hardness to be closely related to the Young's modulus ($E$).[15] $E$ is a measure of a material's resistance to axial stress under circumstances where plastic flow is prohibited. Thus, the atomic movement in glass during axial deformation should be similar to that during elastic deformation during indentation, i.e., $E$ correlates well with the elastic part of indentation, and hence, with hardness under certain circumstances. Recently, Hand and Tadjiev[16] proposed a direct one-to-one relation between $E$ and $H_v$ and found that increasing hardness is usually correlated with increasing modulus. While this correlation applies to many compositions,[16] it does not apply to all.[4,13] Therefore, the intrinsic link between $E$ and $H_v$ still needs to be explored. To the best of our knowledge, the relation between the elastic part of indentation and hardness has not yet been studied.

In this paper, we investigate the correlation between Vickers hardness ($H_v$) and the deformation processes under indentation in a series of mixed magnesium-barium boroaluminosilicate glasses. In our recent investigations on the relation between deformation processes under indentation and $H_v$, we kept $E$ constant and thus neglected its influence on $H_v$.[4,13] Here, we choose a series of boroaluminosilicate glasses with varying MgO/BaO molar ratios as the objects of this study since they are expected to exhibit a relatively large change in $E$ upon Mg-for-Ba substitution.[17] The contributions of densification and plastic flow to indentation are determined using atomic force microscopy (AFM), applying the method developed by Yoshida *et al.*[10] The composition dependences of density ($\rho$), shear modulus ($G$), glass transition temperature ($T_g$), and liquid fragility index ($m$) are also determined, which are useful for interpreting the AFM results. Finally, we discuss the correlations among the deformation processes under indentation, Young's modulus, and hardness.

## EXPERIMENTAL

### Sample preparation

The nominal compositions of the studied mixed magnesium-barium boroaluminosilicate glasses are $64SiO_2$-$12Al_2O_3$-$6B_2O_3$-$12Na_2O$-$(6-x)MgO$-$xBaO$, where $x = 0$, 1.5, 3, 4.5, and 6. The end-member glasses, i.e., $x = 0$ and 6, were previously studied in Refs. 18–20 with respect to their mechanical, thermophysical, and optical properties. All glasses included $\sim 0.16$ mol. % $SnO_2$ as a fining agent. To prepare the glasses, the raw materials were first melted in a covered platinum crucible for 5 h in air at a temperature between 1450 and 1600 °C, depending on composition. The melts were first quenched in water, and the resulting glass pieces were crushed and remelted for 6 h at 1650 °C and finally cast onto a stainless steel plate in air. The remelting was performed to ensure quality and homogeneity of the final glass product. The glasses were annealed for 2 h at their respective annealing points ($\eta = 10^{12.3}$ Pa s). The chemical compositions of the final glasses were determined using X-ray fluorescence, and the analyzed compositions were all within 0.5 mol. % of the nominal targets (see Table I). Room-temperature densities of the glasses were determined by Archimedes' principle using water as immersion liquid.

## Viscosity

The temperature dependence of equilibrium viscosity was measured by performing beam bending, parallel plate, and concentric cylinder experiments. The viscosity curve of each composition is represented by data points at $10^{6.6}$ Pa s (obtained via parallel plate viscometry), $10^{11}$ Pa s (obtained via beam bending viscometry), and 12–20 data points in the range of $10^1$ to $10^6$ Pa s (obtained via the concentric cylinder method). For beam bending experiments, bars of 55 mm length and $2.5 \times 2.5$ mm$^2$ cross section were cut from the bulk glasses. For parallel plate experiments, cylinders of 6.0 mm diameter and 5.0 mm thickness were core drilled, and afterwards, the flats were polished to an optical finish. For concentric cylinder experiments, $\sim 600$ g of crushed glass was remelted. The temperature errors associated with determining the $10^{11}$ Pa s point by the beam-bending method and the $10^{6.6}$ Pa s point by the parallel plate method are $\pm 1$ and $\pm 2$ °C, respectively. The estimated error in viscosity for the high-temperature measurements (by the concentric cylinder method) is $\log(\eta) = \pm 0.02$ ($\eta$ in Pa s).

## Indentation and AFM

All of the prepared glass samples were polished to mirror image finish and $H_v$ was measured using a Duramin 5 indenter (Struers A/S). A total of 30 indents were conducted on each sample using an indentation time of 10 s and an indentation load of 0.49 N. The measurements were performed in air at room temperature. The indentation impressions were observed using a Ntegra (NT-MDT) AFM. Measurements of deformation volumes were performed in tapping mode at 50% relative humidity and room temperature. The AFM cantilever had a silicon tip, the scanning frequency was 0.47 Hz, and the scan size was $20 \times 20$ $\mu m^2$. Following the procedure of Yoshida *et al.*,[10] at least ten indentations were examined before and after annealing for 2 h at 0.9 times the glass transition temperature (in K) of the respective composition.

TABLE I. Chemical compositions of the 5 magnesium-barium boroaluminosilicate glasses under study, which were analyzed using X-ray fluorescence ($\pm 0.1$ mol. %).

| Glass ID | Composition (mol. %) | | | | | | |
|---|---|---|---|---|---|---|---|
| | $SiO_2$ | $Al_2O_3$ | $B_2O_3$ | $Na_2O$ | MgO | BaO | $SnO_2$ |
| Mg-Ba0 | 64.03 | 11.80 | 5.99 | 11.92 | 5.89 | … | 0.15 |
| Mg-Ba1.5 | 64.03 | 11.91 | 6.04 | 11.77 | 4.53 | 1.50 | 0.15 |
| Mg-Ba3 | 64.02 | 11.93 | 6.01 | 11.87 | 2.98 | 2.98 | 0.15 |
| Mg-Ba4.5 | 64.06 | 11.96 | 5.96 | 11.83 | 1.52 | 4.46 | 0.15 |
| Mg-Ba6 | 63.87 | 11.94 | 5.92 | 11.96 | 0.03 | 6.09 | 0.16 |

## Elastic moduli

The elastic properties ($E$ and $G$) were measured at room temperature using resonant ultrasound spectroscopy. Prisms of dimensions $10\,\text{mm} \times 8\,\text{mm} \times 6\,\text{mm}$ were used to gather resonance spectra from 100 to 300 kHz. For each sample, the first five resonant peaks as a function of frequency resulting from excited resonant eigenmodes were used to calculate the elastic properties.

## Calorimetry

Calorimetric measurements were performed on a differential scanning calorimeter (DSC 449C, Netzsch) to determine the calorimetric $T_g$. Each sample was subjected to two up and downscans at 10 K/min to a maximum temperature of $\sim$100 K above the glass transition temperature. The first scan reflects an unknown thermal history, whereas the second scan reflects the standard thermal history of a cooling of 10 K/min.[21] A flow of 40 ml/min argon was used as protective gas, and platinum crucibles were used for both sample and reference. In order to calculate the isobaric heat capacity ($C_p$) of the aluminosilicate glasses, a sapphire standard of approximately the same weight was measured before the measurement of each sample.

## RESULTS

The composition dependence of the elastic moduli ($E$ and $G$) is plotted in Fig. 1 for the mixed Mg-Ba boroaluminosilicate glass series with various molar ratios of [MgO]/([MgO] + [BaO]) (hereafter, this molar ratio is denominated by the symbol $f$). It is seen that $E$ decreases linearly with $f$, whereas $G$ decreases in a nonlinear fashion with the largest deviation from linearity at $f = 0.5$. That is, the mixed alkaline earth effect is observed in $G$, but not in $E$ (Fig. 1). The nonlinear trend for $G$ and the negative linear trend for $E$ have not been reported in earlier studies.[4,13] Using these trends, we can qualitatively explain the changing trend of the elastic part of deformation under indentation with varying $f$. From
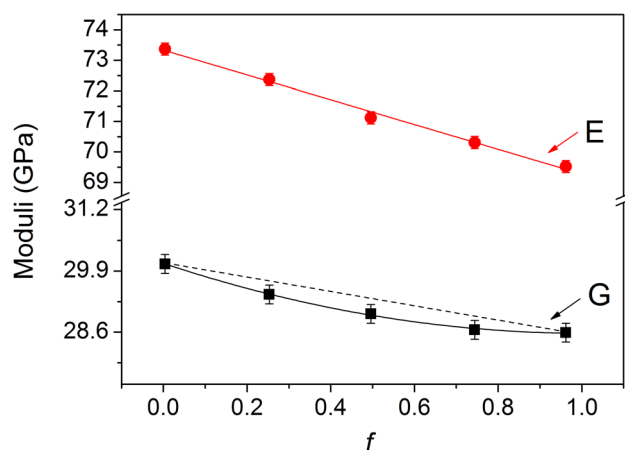


FIG. 2. Poisson's ratio ($\nu$) as a function of the molar ratio of $f = $ [MgO]/([MgO] + [BaO]). $\nu$ is calculated as $2E/G - 1$.[9] The solid line represents the compositional scaling of $\nu$, whereas the dashed line depicts a linear relation between the two end-member compositions. Both lines are guides for the eye.
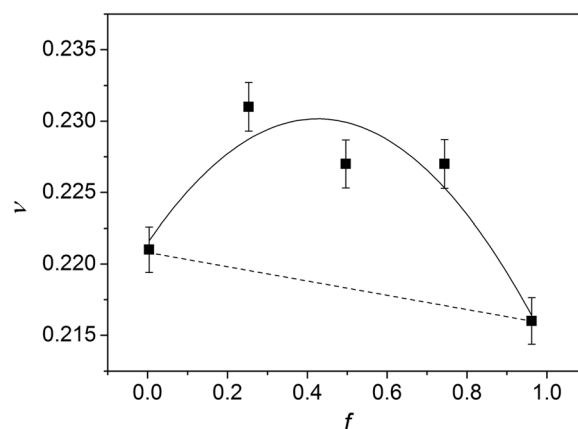
the values of $E$ and $G$, the Poisson's ratio ($\nu$) can be calculated as $\nu = 2E/G - 1$.[9] In Fig. 2, $\nu$ is plotted as a function of $f$. It is seen that $\nu$ initially increases with $f$ and then decreases when $f > 0.5$, i.e., the largest deviation from linearity is found at $f = 0.5$.

Fig. 3 shows the composition dependence of $H_v$, which manifests an initial increase followed by a decrease with $f$, i.e., the mixed alkaline earth effect of hardness occurs. The largest negative deviation from linearity and the minimum value of $H_v$ are observed at around $f = 0.5$. Examples of the indents are shown in Fig. 4. As mentioned in the introduction, the resistance of a glass to deformation during Vickers indentation is a result of three distinct processes, namely, plastic flow, densification, and elastic deformation.[9] AFM measurements are therefore performed to determine the size of the indents and the amount of pile-up both before and after sub-$T_g$ annealing. From these results, the volume of densification ($V_d$) and volume of plastic flow ($V_p$) are calculated as per Eqs. (1) and (2):[10]
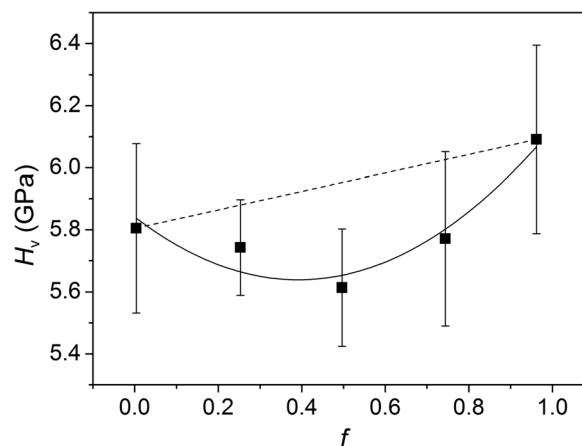


FIG. 1. Shear modulus ($G$) and Young's modulus ($E$) as a function of the molar ratio ($f$) of magnesium to total alkaline earth content, i.e., [MgO]/([MgO] + [BaO]). The solid lines represent the compositional scaling of $E$ and $G$, whereas the dashed lines depict a linear relation between the two end-member compositions. Both lines are guides for the eye.



FIG. 3. Vickers hardness ($H_v$) as a function of the molar ratio of $f = $ [MgO]/([MgO] + [BaO]). The solid line represents the compositional scaling of $H_v$, whereas the dashed line depicts a linear relation between the two end-member compositions. Both lines are guides for the eye.
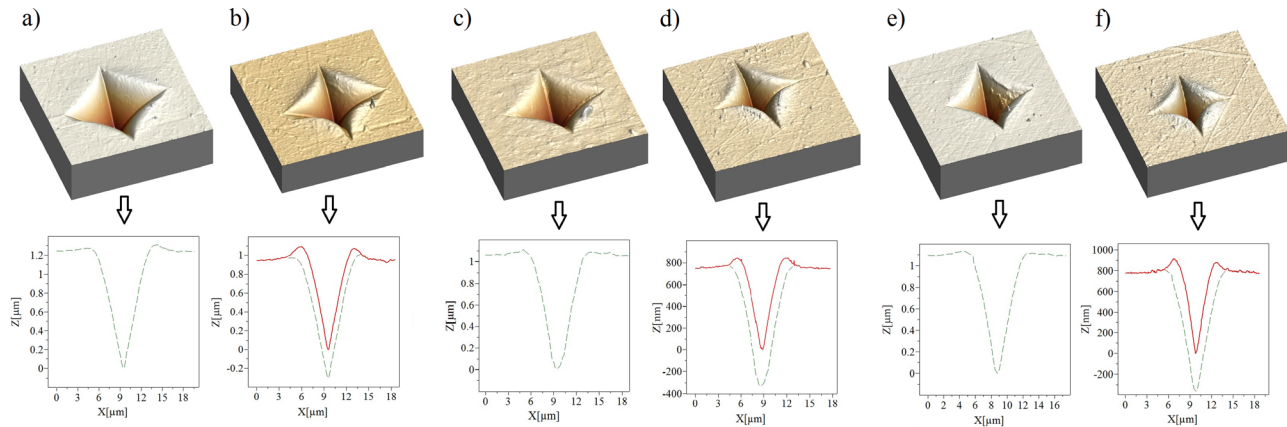
a)    b)    c)    d)    e)    f)



FIG. 4. AFM images of indents and their respective cross-sections. Images (a) and (b) are obtained for the glass with $f = 0$ before and after annealing at $0.9 \times T_g$ (in K), respectively. Images (c) and (d) are for the glass with $f = 0.5$ before and after annealing at $0.9 \times T_g$, respectively. Images (e) and (f) are obtained for the glass with $f = 1$ before and after annealing at $0.9 \times T_g$, respectively. All images have the same scanning area ($20\,\mu m \times 20\,\mu m$), but the height of the images (z) is different and indicated on each cross-sectional image. The dashed lines represent the initial volume ($V_i^-$), while the solid lines indicate the indent volume after annealing ($V_i^+$). The volume in between is the volume of densification ($V_d$).

$$V_d = (V_i^- - V_a^-) + (V_a^+ - V_i^+), \qquad (1)$$

$$V_p = V_i^- - ((V_i^- - V_a^-) + (V_a^+ - V_i^+)), \qquad (2)$$

where subscripts $i$ and $a$ indicate initial volumes and volumes after annealing, respectively, and superscripts $-$ and $+$ indicate indentation volumes and pile-up volumes, respectively. The derived volumes of densification and plastic flow ($V_d$ and $V_p$) are plotted in Fig. 5 as a function of $f$, and their determination is illustrated in Fig. 4. Both $V_d$ and $V_p$ exhibit nonlinear compositional scaling with the largest deviation from linearity at around $f = 0.5$. $V_p$ is experiencing a positive deviation, while $V_d$ is experiencing a negative deviation from linearity, but both exhibit the mixed alkaline earth effect. It is notable that $V_d$ is ~4 times larger than $V_p$.

The Poisson's ratio is a measure of the materials ability to expand in the transverse axes of applied compression, and is consequently closely related to $V_d$ and $V_p$. A negative correlation has previously been proposed between $\nu$ and the ratio of densification to initial indentation volume (this ratio is

also referred to as the volume of recovery ($V_R$)).[10,22] To test this, the volume of recovery is plotted as a function of magnesium to total alkaline earth content in Fig. 6. $V_R$ initially decreases with $f$, but at around $f = 0.5$, the slope changes and $V_R$ increases with further increase in $f$. The compositional scaling of $V_R$ (Fig. 6) resembles that of $1/\nu$ (Fig. 2).

The composition dependence of liquid fragility index ($m$) and glass transition temperatures ($T_g$) both relates to shear motion and thus to plastic flow. To determine the liquid fragility index, $m$, we use the measured viscosity data in the range of $10^1$ to $10^{11}$ Pa s. Those data are fitted to the equation:[23]

$$\log \eta(T) = \log \eta_\infty + (12 - \log \eta_\infty)$$
$$\times \frac{T_g}{T} \exp\left[\left(\frac{m}{12 - \log \eta_\infty} - 1\right)\left(\frac{T_g}{T} - 1\right)\right], \quad (3)$$

where $\eta_\infty$ is the high-temperature limit of liquid viscosity. The derived $m$ values are plotted against composition in
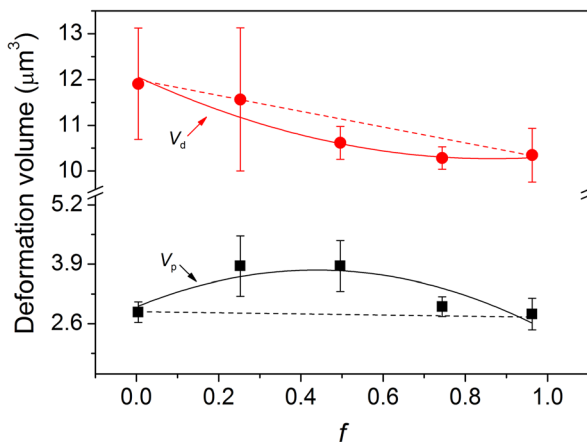


FIG. 5. Volumes of plastic flow ($V_p$) and densification ($V_d$) as a function of the molar ratio of $f = [MgO]/([MgO] + [BaO])$. The solid lines represent the compositional scaling of $V_p$ and $V_d$, whereas the dashed lines depict a linear relation between the two end-member compositions. Both lines are guides for the eye.
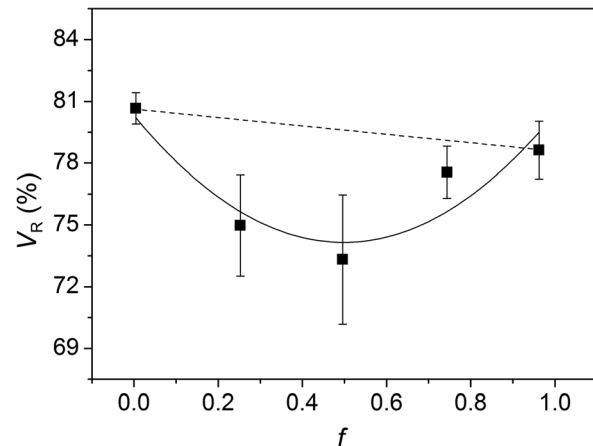


FIG. 6. Volume of recovery ($V_R$) as a function of the molar ratio of $f = [MgO]/([MgO] + [BaO])$. The solid line represents the compositional scaling of $V_R$, whereas the dashed line depicts a linear relation between the two end-member compositions. Both lines are guides for the eye.
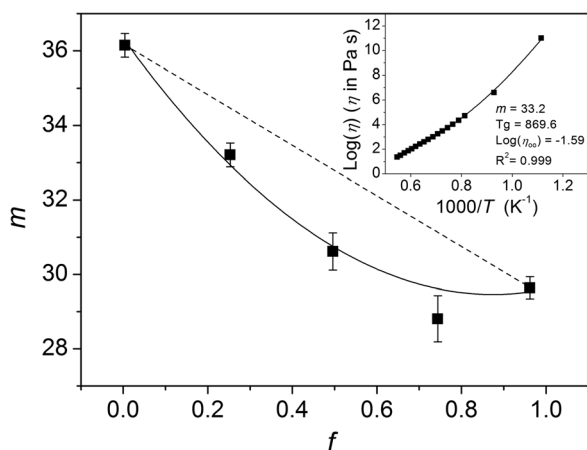
FIG. 7. Liquid fragility indices ($m$) as a function of the molar ratio of $f = [MgO]/([MgO] + [BaO])$. $m$ values are determined by fitting Eq. (3) to viscosity data. An example of this determination is shown in the inset,[20] where $f = 0.75$ is used as an example. The solid lines represents the compositional scaling of $m$, whereas the dashed line depicts a linear relation between the two end-member compositions. Both lines are guides for the eye.



FIG. 9. Density ($\rho$) and molar volume ($V_0$) as a function of the molar ratio of $f = [MgO]/([MgO] + [BaO])$. $\rho$ is plotted on the primary ordinate and $V_0$ on the secondary. The solid lines represent the compositional scaling of $\rho$ and $V_0$, whereas the dashed line depicts a linear relation between the two end-member compositions. Both lines are guides for the eye.

Fig. 7. The $T_g$ values determined by DSC are shown in Fig. 8, and experience similar compositional scaling as those obtained from Eq. (3). It is seen in Fig. 7 that $m$ experiences a nonlinear decrease with increasing $f$, and on Fig. 8 that $T_g$ experiences a nonlinear increase with increasing $f$. Both $T_g$ and $m$ have the largest deviation from linearity at $f \approx 0.5$.

Fig. 9 shows the compositional scaling of $\rho$ and molar volume ($V_0$). $V_0$ is calculated as the molar mass divided by the glass density. $\rho$ is found to linearly decrease with $f$, whereas $V_0$ decreases in a nonlinear fashion with the largest deviation from linearity at $f \approx 0.5$.

## DISCUSSION

### Elastic deformation

Based on the information of the short-range glass structure, such as interatomic bonding energies and network connectivity, it is possible to estimate the composition dependence of
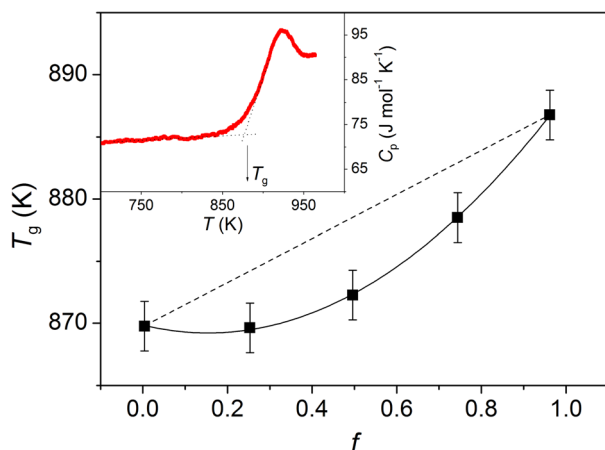


FIG. 8. Glass transition temperatures ($T_g$) as a function of the molar ratio of $f = [MgO]/([MgO] + [BaO])$. The solid line represents the compositional scaling of $T_g$, whereas the dashed line depicts a linear relation between the two end-member compositions. Both lines are guides for the eye. Inset: Determination of $T_g$, using the glass with $f = 0.25$ as an example.[21]
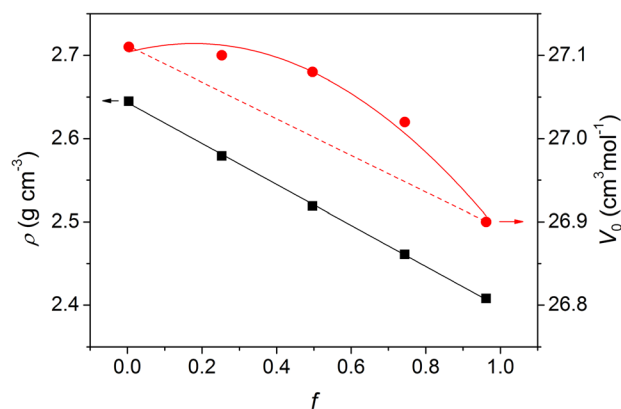
properties such as $E$ and $H_v$.[1,11,15,24,25] Therefore, it could be expected that the two properties are linked since they rely on the same set of underlying constraints.[9,15,16] Hand and Tadjiev[16] found a relatively good positive correlation between $E$ and $H_v$ for a wide range of glasses ($R^2 = 0.74$). In this work, $E$ exhibits a linear decrease with increasing $f$ (Fig. 1), whereas $H_v$ exhibits a minimum value at $f = 0.5$ and a general increase from the Mg to Ba end-member compositions (Fig. 3). Thus, for the mixed alkaline earth glasses investigated in this study, there is not a positive correlation between $E$ and $H_v$. Consequently, if $E$ is considered to represent the resistance to elastic deformation under indentation, elastic deformation is not the dominant deformation process when predicting the mixed alkaline earth effect of hardness. If the composition dependence $H_v$ is primarily controlled by the resistance to elastic deformation, it would be expected that the observed linear decrease in $E$ would be superimposed on $H_v$. However, this is not the case as $H_v$ generally increases with increasing $f$ (i.e., not decreases as observed for $E$).

### Densification

$\rho$ (Fig. 9) exhibits the same compositional trend as $E$ (Fig. 1), i.e., a linear decrease with increasing $f$, in consistence with the trend reported in Ref. 26. As MgO has a smaller molar mass than BaO, the decrease in $\rho$ can be attributed to the substitution of $Mg^{2+}$ ions for $Ba^{2+}$ in former barium sites within the glassy network. This coincides with the general decrease in $V_0$ (Fig. 9) and $E$ (Fig. 1), assuming that the Mg sites are essentially similar to the Ba sites.[26] Both density and refractive index have been used as indicators for the amount of densification ($V_d$) that occurs during indentation.[1,27] Within a family of glasses, as the density increases, the resistance towards densification intuitively becomes larger and the relative amount of densification therefore decreases. However, this is not the case for the glasses in this study. As $f$ increases, $\rho$ decreases, and thus, $V_d$ would be expected to increase. However, on the contrary, an inverse relation is observed as shown in Fig. 5. The same inverse relation is observed for the bulk modulus (calculated from $E$

and $G$), as it decreases with increasing $f$. This means that $V_d$ does not positively correlate with either bulk modulus (Fig. 1) or $\rho$ (Fig. 9). Both $V_d$ (Fig. 5) and $V_R$ (Fig. 6) exhibit negative deviations from linearity, corresponding to a positive deviation in the resistance to densification. Assuming that densification is the dominant deformation process, $H_v$ would be expected to positively deviate from linearity. In Fig. 3, it is seen that this is not the case.

It is worth mentioning that the investigated glasses, compared to, e.g., aluminosilicates, might undergo a larger degree of densification because boron could be converted from trigonal to tetrahedral configuration during indentation.[28,29] This conversion results in an increased density of the network, enhancing the effect of densification on hardness. However, the larger degree of densification in the boron-containing glasses compared to that of boron-free glasses is not observed, since $V_R$ of the studied glasses (Fig. 6) is generally lower than that of a mixed Na/K aluminosilicate system without boron.[30] As no correlation is observed between $V_d$ and $H_v$, we infer that densification is not the dominant deformation process during indentation of the studied glasses.

### Plastic flow

$G$ (Fig. 1), $H_v$ (Fig. 3), and $V_p$ (Fig. 5) are related to structural shear motion, and show a mixed alkaline earth effect.[16,31] $m$ (Fig. 7) and $T_g$ (Fig. 8) are dynamic quantities that relate to the viscosity of the glass, and they also exhibit a mixed alkaline earth effect. It has recently been proposed that in mixed modifier aluminosilicate glasses, plastic deformation is the dominant part of the total deformation,[4,13] and thus, the dominant factor in determining the compositional dependence of $H_v$. As known, $G$, $m$, and $T_g$ all exhibit a negative mixed alkaline earth effect with largest deviation from linearity around $f = 0.5$. Hence, when both types of the alkaline earth ions co-exist in the glass, the resistance of the glass to deformation will be lowest because of the largest negative deviation from the linear trend of plastic flow. $V_p$ undergoes a positive mixed alkaline earth effect, implying that the positive deviation of both shear and plastic flow from a linear trend reaches the highest degree near $f = 0.5$. This is in good agreement with the measured compositional scaling of hardness, and the findings presented in Ref. 4. The dominant role of plastic flow in determining the mixed alkaline earth effect on the glass hardness is verified by the measured composition dependence of indentation volumes (Fig. 5). Assuming a linear positive relation between deformation resistances and indentation volumes, the resistance of the glass to plastic flow should be four times larger than that to densification, since the value of $V_p$ is four times smaller than that of $V_d$. In addition, it is interesting to note that the mixed alkaline earth effect is found for $G$, but not for $E$ (Fig. 1). This confirms that plastic shear flow is the controlling deformation process for the compositional scaling of hardness, because $G$ is inversely proportional to the degree of shear motion, whereas $E$ negatively relates to the compactness of the glass.[32] The compositional trends of $G$ and $E$ are reflected in the compositional behavior of $\nu$ (Fig. 2).

As the compositional changes in $E$ do not affect $H_v$, the resistance of the glass to elastic deformation is believed to be rather small compared to the resistance to plastic flow. As the indenter penetrates the glassy material, all three deformation modes co-act, but the one with the highest resistance to the external load is the dominant one in determining the glass hardness.[9] Hence, lowering the highest resistance of the deformation mode to the external load should affect the glass hardness the most, in agreement with the theory proposed by Yamane and Mackenzie,[9] according to which $H_v$ is proportional to the geometrical average of the three resistances. Although plastic flow is the dominant deformation process, a quantitative link between plastic flow and Vickers hardness has not yet been established. This means that the degree of plastic flow exerts a much larger influence on Vickers hardness compared to that of both densification and elastic deformation. However, it is still not possible at this stage to predict the absolute hardness values solely from the plastic flow volumes.

### Poisson's ratio

An alternative way to explain the compositional scaling of $H_v$ is to explore the change of $\nu$ with composition. A general rule has been proposed to account for the relation between $\nu$ and $V_R$ in glassy materials,[1,10] viz., an increase in $\nu$ results in a decrease in $V_R$. For small changes in $\nu$, which is the case in this study (Fig. 2), the relation can be approximated by a linear scaling. That is, the tendency of the change of $\nu$ with composition corresponds to the inverse trend of $V_R$. This agrees with the results displayed in Figs. 2 and 6, where the observed compositional minimum in $\nu$ corresponds to the observed maximum in $V_R$. As mentioned earlier, the ratio between the deformation processes during indentation differs between different families of glasses, and any correlation between $\nu$ and $H_v$ is thus not universal, as $H_v$ does not correlate with the elastic part of indentation. Since $\nu$ relates to the ratio between transverse and axial strain, it is a viable index to discriminate between densification and plastic flow.[1] Higher values of $\nu$ correspond to a larger ratio of transverse to axial strain, and therefore, plastic flow is favored. Within the same glass series, e.g., mixed modifier silicate glasses, a correlation between the dominant deformation mechanism and $H_v$ has been found to exist.[4,13] As observed in this work, within a given family of glasses, a correlation exists between $\nu$ and $H_v$.

### CONCLUSIONS

In the investigated series of magnesium-barium boroaluminosilicate glasses, we have found that the mixed alkaline earth effects manifest themselves as deviations from linearity in shear modulus ($G$), Poisson's ratio ($\nu$), Vicker's hardness ($H_v$), volume of densification ($V_d$), volume of plastic flow ($V_p$), volume recovery of indentation ($V_R$), glass transition temperatures ($T_g$), liquid fragility indices ($m$), and molar volume ($V_0$). We found that $E$ and $\rho$ do not exhibit a mixed alkaline earth effect, but exhibit linear composition dependence. We found no correlation between the observed compositional

trends of $E$ and $H_v$. Since $E$ represents the elastic part of indentation resistance, we infer that the elastic deformation does not play the dominant role in determining the mixed alkaline earth effect of hardness in mixed magnesium-barium boroaluminosilicate glasses. Instead, we confirm that plastic flow is the dominant deformation process during indentation of mixed modifier glasses.

Interestingly, we have also found that Poisson's ratio exhibits a positive deviation from compositional linear dependence, which is in agreement with the negative deviation from linearity observed in hardness. Higher values of Poisson's ratio correspond to a higher degree of shear and a higher volume of plastic flow, and thus, Poisson's ratio is negatively correlated to hardness in cases where either densification or plastic flow have the largest impact on glass hardness.

[1]T. Rouxel, J. Ji, J. P. Guin, F. Augereau, and B. Rufflé, J. Appl. Phys. **107**, 094903 (2010).

[2]W. B. Hillig, "Concerning the creation and stability of pyramidal hardness impression on glass," in *Proceedings of the VIth International Congress on Glass*, Washington, 8–14 July 1962 (American Ceramic Society, Westerville, OH, 1963), p. 51.

[3]E. W. Taylor, Nature **163**, 323 (1949).

[4]J. Kjeldsen, M. M. Smedskjaer, J. C. Mauro, and Y. Z. Yue, Appl. Phys. Lett. **104**, 051913 (2014).

[5]F. M. Ernsberger, J. Am. Ceram. Soc. **51**, 545 (1968).

[6]K. W. Peter, J. Non-Cryst. Solids **5**, 103 (1970).

[7]D. M. Marsh, Proc. R. Soc. A **282**, 33 (1964).

[8]A. K. Varshneya, Int. J. Appl. Glass Sci. **1**, 131 (2010).

[9]M. Yamane and J. D. Mackenzie, J. Non-Cryst. Solids **15**, 153 (1974).

[10]S. Yoshida, J.-C. Sanglebæuf, and T. Rouxel, J. Mater. Res. **20**, 3404 (2005).

[11]J. E. Neely and J. D. Mackenzie, J. Mater. Sci. **3**, 603 (1968).

[12]T. Rouxel, J. C. Sanglebæuf, C. Moysan, and B. Truffin, J. Non-Cryst. Solids **344**, 26 (2004).

[13]J. Kjeldsen, M. M. Smedskjaer, J. C. Mauro, R. E. Youngmann, L. Huang, and Y. Z. Yue, J. Non-Cryst. Solids **369**, 61 (2013).

[14]M. Jebahi, D. André, F. Dau, J. Charles, and I. Iordanoff, J. Non-Cryst. Solids **378**, 15 (2013).

[15]A. Makishima and J. D. Mackenzie, J. Non-Cryst. Solids **12**, 35 (1973).

[16]R. J. Hand and D. R. Tadjiev, J. Non-Cryst. Solids **356**, 2417 (2010).

[17]R. Kirchheim, J. Non-Cryst. Solids **328**, 157 (2003).

[18]M. M. Smedskjaer and M. Potuzak, J. Am Ceram. Soc. **96**, 2831 (2013).

[19]M. Potuzak and M. M. Smedskjaer, Phys. Chem. Glasses: Eur. J. Glass Sci. Technol. B **55**, 18 (2014).

[20]M. M. Smedskjaer, M. Potuzak, X. Guo, and J. C. Mauro, Opt. Mater. **35**, 2435 (2013).

[21]Y. Z. Yue, J. D. Christiansen, and S. L. Jensen, Chem. Phys. Lett. **357**, 20 (2002).

[22]P. Sellappan, T. Rouxel, F. Celarie, E. Becker, P. Houizot, and R. Conradt, Acta Mater. **61**, 5949 (2013).

[23]J. C. Mauro, Y. Z. Yue, A. J. Ellison, P. K. Gupta, and D. C. Allan, Proc. Natl. Acad. Sci. U.S.A. **106**, 19780 (2009).

[24]Q. Zheng, M. Potuzak, J. C. Mauro, M. M. Smedskjaer, R. E. Youngman, and Y. Z. Yue, J. Non-Cryst. Solids **358**, 993 (2012).

[25]M. M. Smedskjaer, J. C. Mauro, and Y. Z. Yue, Phys. Rev. Lett. **105**, 115503 (2010).

[26]N. Soga, H. Yamanaka, C. Hisamoto, and M. Kunugi, J. Non-Cryst. Solids **22**, 67 (1976).

[27]T. Rouxel, H. Ji, T. Hammouda, and A. Moréac, Phys. Rev. Lett. **100**, 225501 (2008).

[28]L. S. Du, J. R. Allwardt, B. C. Schmidt, and J. F. Stebbins, J. Non-Cryst. Solids **337**, 196 (2004).

[29]A. Winterstein-Beckmann, D. Moncke, D. Palles, E. I. Kamitsos, and L. Wondraczek, J. Non-Cryst. Solids **401**, 110 (2014).

[30]J. Kjeldsen, M. M. Smedskjaer, J. C. Mauro, and Y. Z. Yue, J. Non-Cryst. Solids **406**, 22 (2014).

[31]Y. Hasegawa, Glastech. Ber. **57**, 177 (1984).

[32]T. Rouxel, C. R. Mec. **334**, 743 (2006).